Appl. Chem. Eng., Vol. 27, No. 4, August 2016, 421-426
http://dx.doi.org/10.14478/ace.2016.1062

Article

전기화학 증착법에 의해 합성된 폴리옥소메탈레이트/폴리피롤/탄소천 전극의 전기화학적 특성

윤조희 · 최봉길†

강원대학교 화학공학과
(2016년 6월 30일 접수, 2016년 7월 11일 심사, 2016년 7월 11일 채택)

Electrochemical Characteristics of Polyoxometalate/Polypyrrole/Carbon Cloth Electrode Synthesized by Electrochemical Deposition Method

Jo Hee Yoon and Bong Gill Choi†

Department of Chemical Engineering, Kangwon National University, 346 Joongang-ro, Samcheok, Gangwon-do 25913, South Korea
(Received June 30, 2016; Revised July 11, 2016; Accepted July 11, 2016)

초 록

본 연구에서는 폴리옥소메탈레이트(polyoxometalate, POM)가 도핑된 폴리피롤(polypyrrole, Ppy)을 3차원 구조의 탄소천(carbon cloth, CC) 표면 위에 전기화학적 증착법을 이용하여 합성하고 이의 의사커패시터 특성을 순환전압전류법과 정전류 충전-방전법을 사용하여 분석하였다. POM-Ppy의 코팅은 전기화학적 증착 시간에 따라서 얇은 conformal형태의 코팅으로 조절되었다. 제조된 POM-Ppy/CC의 재료 특성은 전자주사현미경과 X-선 분광분석을 사용하여 분석하였다. POM-Ppy/CC의 3차원 나노복합체 구조는 높은 비정전용량(561 mF/cm^2), 고속 충방전(85% 용량 유지율) 및 장수명 특성(97% 용량 유지율)을 나타내었다.

Abstract

In this report, polyoxometalte (POM)-doped polypyrrole (Ppy) was deposited on surface of three-dimensional carbon cloth (CC) using an electrodeposition method and its pseudocapacitive behavior was investigated using cyclic voltammetry and galvanostatic charge-discharge. The POM-Ppy coating was thin and conformal which can be controlled by electrodeposition time. As-prepared POM-Ppy/CC was characterized using scanning electron microscope and energy-dispersive X-ray spectroscopy. The unique 3D nanocomposite structure of POM-Ppy/CC was capable of delivering excellent charge storage performances: a high areal capacitance (561 mF/cm^2), a high rate capability (85%), and a good cycling performance (97% retention).

Keywords: *polyoxometalate, polypyrrole, pseudocapacitor, nanocomposite, electrochemical performance*

1. Introduction

Pseudocapacitors accumulate electrical charges using fast and reversible faradic redox reactions of conducting polymers and metal oxides (or hydroxides) as electrode materials[1-5]. These pseudocapacitive materials are capable of delivering higher theoretical capacitance compared to carbon-based electrode materials which are widely used electrical double layer capacitors[6,7]. For instance, hydrous ruthenium oxide-based electrodes were reported to achieve as high as specific capacitance of 1200 F/g using aqueous electrolytes[8]. Despite this remarkable performance, the relative high cost of ruthenium for the preparation of ruthenium-based electrode materials limits their widespread applications. In this regard, conducting polymers, such as polyaniline and polypyrrole, have attracted great of attention as alternative materials to conventional activated carbons because of their high theoretical capacitances, high electrical conductivity, low cost, and environmental friendliness[9-12]. Although conducting polymers provide high theoretical capacitance values, conducting polymer-based electrodes suffer from poor cyclic stability due to mechanical degradation during the doping/dedoping process over long periods of time[9-12].

To address this issue, a number of studies have been attempted, including well-controlled nanostructures of conducting polymers, hybridization with carbon materials, and development of anionic dopants[13-17]. In particular, the employment of advanced anionic dopants for polymerization of conducting polymers have influenced electrical conductivity, morphology, and redox reaction behavior during electrochemical reactions, resulting in enhanced long-term stability. Zhitomirsky *et al.* synthesized sulfanilic acid azochromotrop-doped polypyrrole electrode mate-

† Corresponding Author: Kangwon National University,
Department of Chemical Engineering, 346 Joongang-ro, Samcheok, Gangwon-do 25913, South Korea
Tel: +82-33-570-6545 e-mail: bgchoi@kangwon.ac.kr

pISSN: 1225-0112 eISSN: 2288-4505

rials, showing 91.5% capacitance retention after 1000 cycles[18]. Same group improved cycle life of pseudocapacitors based on tiron-doped polypyrrole electrodes[19]. However, these acidic dopants are toxic, and thus are limited to commercial use in preparation of electrode materials.

Polyoxometalates (POMs) are anionic metal oxide cluster at nanoscale and are considered promising candidates for preparing electrochemical electrodes in applications of water splitting, sensors, and energy conversion and storage due to their multiple redox properties, thermal stability, and electron/proton transfer (or storage) abilities[20-22]. Compared to other dopants, POMs could accumulate electrical charges through redox reactions, resulting in high theoretical values for supercapacitor applications. Some of the studies have been attempted to incorporate POMs into conducting polymer matrixes. Gómez-Romero *et al.* described preparation of POM-incorporated conducting polymer nanocomposites based on their strong electrostatic interactions. This study showed high specific capacitances of 120 F/g for POM-doped polyaniline[23]. Freund *et al.* reported a higher specific capacitance (210 F/g) for pseudocapacitors based on porous structure of POM-doped polypyrrole electrodes[24]. The porous structure enabled efficient and rapid ion transfer, and thus improved electrochemical performances. McCormac *et al.* reported POM-entrapped polypyrrole through electrochemical deposition of POMs during electropolymerization of pyrrole monomers[25]. Although the electrochemical method is simple and effective for incorporation of POMs into conducting polymers, no reports have yet described on the development of pseudocapacitors using POM-doped conducting polymers deposited on porous carbon structures.

Herein, we report a simple and efficient method for the preparation of three-dimensional (3D) POM-doped polypyrrole (Ppy)-deposited on carbon cloth (CC) through an electrochemical deposition process. The coating of POM-Ppy was optimized by deposition time for chronoamperometry. The POM-Ppy continuously coated to the 3D CC surface. In this architecture of POM-Ppy/CC, the POM-Ppy produced multiple and redox reactions at the surface of 3D CC, while 3D CC supported rapid ion and electron transfer. When evaluating electrochemical performances, the POM- Ppy/CC exhibited high areal capacitance, high rate capability, and long-term cycling stability.

2. Experimental

2.1. Materials

All chemicals were commercially available and used without further purification. Phosphomolybdic acid hydrate ($H_3PMo_{12}O_{40} \cdot xH_2O$, denoted POM) and pyrrole (98%) were obtained from Sigma-Aldrich. H_2SO_4 (95%) was purchased from Junsei Chemical Co., Ltd. The deionized (DI) water (18.2 MΩ cm, Millipore Milli Q water system) was used in all experiments.

2.2. Preparation of POM-Ppy/CC

The POM-Ppy/CC was prepared by an electrochemical deposition method using a chronoamperometric technique by a VersaSTAT 4 (Princeton Applied Research) potentiostat. A constant potential of +0.65 V vs. Ag/AgCl was applied for different deposition times to obtain optimized POM-Ppy/CCs. The electrolyte solution for POM-PPy electroplating was prepared by mixing 7 mM of pyrrole monomer and 5 mM of POM dispersed in DI water. After electrodeposition, the POM-Ppy/CCs were washed several times with ethanol and DI water and then dried at 60 ℃ under vacuum.

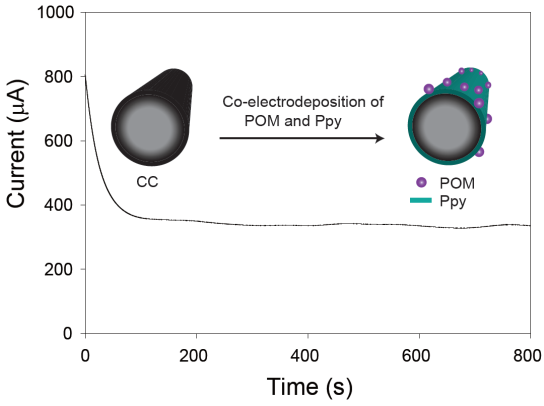

Figure 1. A chronoamperometic curve for electrochemical deposition of POM-Ppy on CC. Inset is scheme of co-electrodepoistion of POM and Ppy on carbon fiber.

2.3. Electrochemical measurements

All of electrochemical measurements, including cyclic voltammetry (CV) and galvanostatic charge/discharge, were conducted on a VersaSTAT 4 (Princeton Applied Research) using a conventional three-electrode system. The Pt wire and an Ag/AgCl electrode were used as the counter and reference electrode, respectively. The electrolyte used is a 1 M H_2SO_4 aqueous solution. In order to evaluate supercapacitor performance, CV tests were carried out at various scan rates from 10 to 100 mV/s. Galvanostatic charge/discharge measurements were made at current densities from 1 to 30 mA/cm^{-2}. Cycle life performance was tested using galvanostatic charge/discharge measurements at a constant current density of 1 mA/cm^{-2} over 1000 cycles.

3. Result and Discussion

POM-Ppy/CCs were typically fabricated by co-electrochemical deposition of POM and Ppy on carbon fiber surface of CC (Inset of Figure 1). A chronoamperometric technique allowed to incorporation of POMs into Ppy during electrochemical polymerization of pyrrole monomers. Figure 1 shows a typical chronoamperometric curve for preparation of POM-Ppy/CC samples. The current decays with reaction time, which is according to the Cottrell behavior as a result of natural convection effects and coupled chemical reactions. After co-electrodeposition of POM and Ppy, black color of CC changed to dark green. The POM-Ppy/CCs shows the excellent mechanical flexibility, and after bending, twisting, or folding they retains their original state without any cracks or damage. The coating of POM-Ppy was optimized by deposition time for a chronoamperometric process (Figure 1). Scanning electron microscope (SEM) images of Figure 2 showed the coating

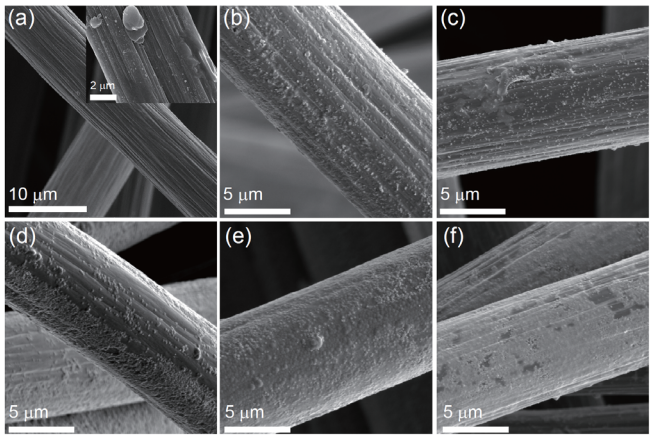

Figure 2. SEM images of POM-Ppy/CC obtained from different deposition times of (a) 0 s, (b) 100 s, (c) 200 s, (d) 500 s, (e) 700 s, and (f) 1000 s. Inset is SEM image of Ppy/CC.

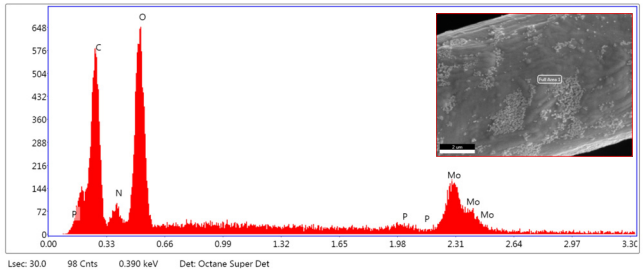

Figure 3. EDX analysis of POM-Ppy/CC.

morphology of POM-Ppy/CCs with different deposition times ranging from 100 to 1000 s. Figure 2a showed bare CC sample composed of interconnected 3D carbon fibers. As the coating time increased, POM-Ppy gradually deposited and covered the surface of CC. Ppy/CC sample without POMs showed similar morphology of POM-Ppy/CC (Inset of Figure 1a). Low-cost CC has been extensively used in energy storage and conversion applications as electrode substrate (*i.e.*, current collectors) to support electrochemical active materials[26,27]. CC provides 3D large surface area POM-Ppy coating roughed the surface of the carbon fibers of CC. The thin and conformal coating of POM-Ppy layers was observed. Energy dispersive X-ray spectroscopy (EDX) analysis confirmed the presence of Mo, P, and O elements for POMs and C and N elements for Ppys (Figure 3). In addition, atomic ratio of Mo element was 43.03 wt% in POM-Ppy/CC (Table 1).

In order to optimize deposition time, CV measurement for POM-Ppy/CCs was performed under a three-electrode system (Figure 4). CV is a useful technique for characterizing the electrochemical and capacitive behavior; area of current density and shape of CV in anodic and cathodic directions. All CV curves showed three-redox peaks in a potential range of -0.1 to 0.9 V due to the multiple redox properties of POMs. The three reversible redox reactions are according to the following equations[28]:

$$PMo_{12}O_{40}^{3-} + 2e^- + 2H^+ \leftrightarrow H_2PMo_{12}O_{40}^{3-} \quad (1)$$

Table 1. Elemental Weight Ratio of POM-Ppy/CC

Element	C K	N K	O K	P K	Mo L
Weight (%)	22.56	6.67	25.76	1.98	43.03

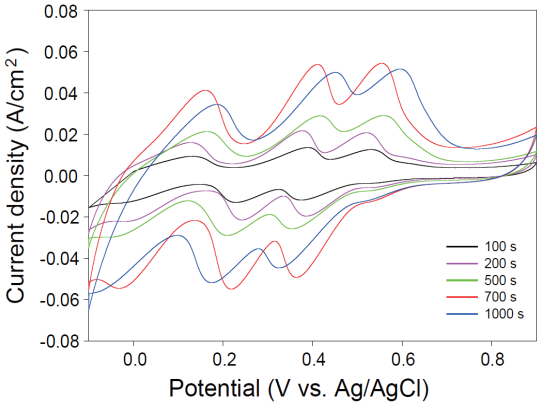

Figure 4. CV curves of POM-Ppy/CCs obtained from different deposition times of 100-1000 s.

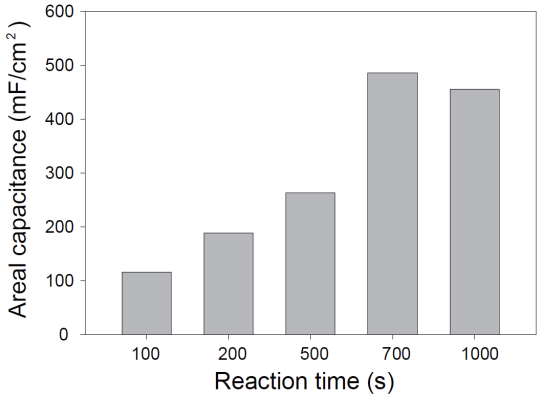

Figure 5. Areal capacitance values of POM-Ppy/CCs obtained from different deposition times of 100-1000 s.

$$H_2PMo_{12}O_{40}^{3-} + 2e^- + 2H^+ \leftrightarrow H_4PMo_{12}O_{40}^{3-} \quad (2)$$

$$H_4PMo_{12}O_{40}^{3-} + 2e^- + 2H^+ \leftrightarrow H_6PMo_{12}O_{40}^{3-} \quad (3)$$

The areal capacitance of POM-Ppy/CCs was evaluated from the CV curves using the following equation[4]:

$$C = \int i dV/(2Av\triangle V) \quad (4)$$

where i is the current (A), $\int i dV$ is the integration area for the CV curves, v is the scan rate (V/s), A is the area (cm^2) of electrode, $\triangle V$ is the potential window (V). When depositing POM and Ppy during 700 s, we obtained maximum specific capacitance of 486 mF/cm^2 for POM-Ppy/CC (Figure 5). In this work, we selected deposition time of 700 s and further characterized the POM-Ppy/CC sample synthesized at deposition time of 700 s.

Figure 6a shows the CV curves of a typical POM-Ppy/CC and

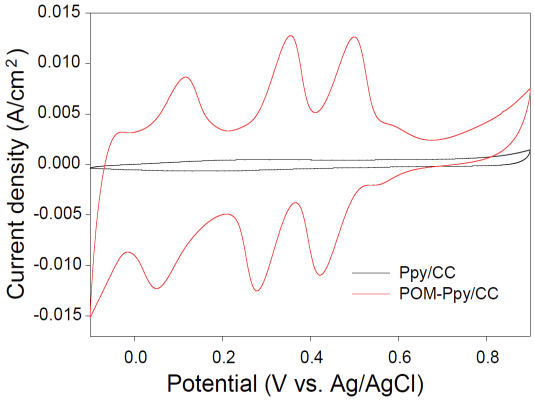

(a)

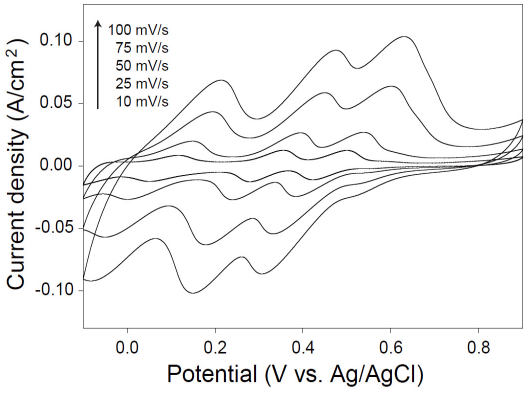

(b)

Figure 6. (a) CV curves of Ppy/CC and POM-Ppy/CC measured at scan rate of 50 mV/s. (b) CV curves of POM-Ppy/CC measured at different scan rates of 10, 25, 50, 75, and 100 mV/s.

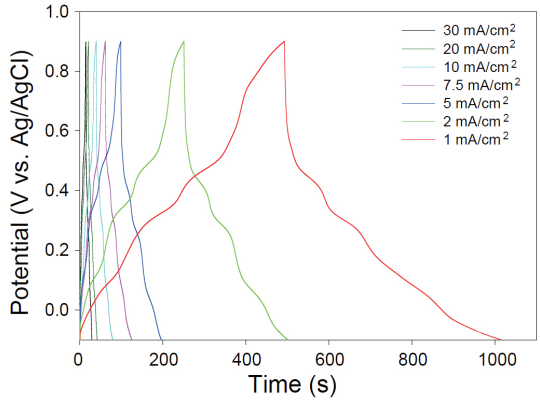

(a)

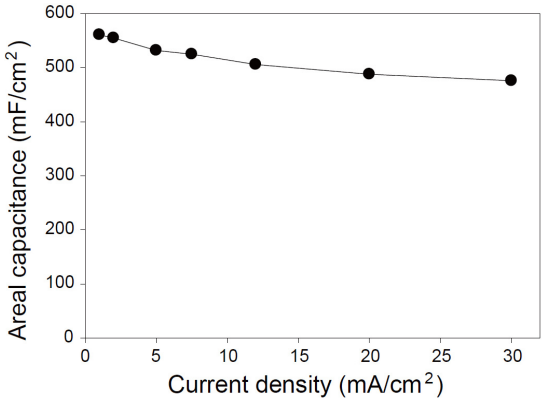

(b)

Figure 7. (a) Galvanostatic charge-discharge curves of POM-Ppy/CC measured at different current densities of 1, 2, 5, 7.5, 10, 20, and 30 mA/cm^2. (b) Areal capacitance values of POM-Ppy/CC calculated with different current densities of 1-30 mA/cm^2.

Ppy/CC electrodes in 1 M Na_2SO_4 aqueous electrolyte. Compared to Ppy/CC, POM-Ppy/CC obviously showed tree characteristic redox peaks, which were attributed to the phosphomolybdate anion being progressively reduced/oxidized. Area of CV curve for POM-Ppy/CC was much higher than that of Ppy/CC, indicating higher specific capacitance. The CV analysis of POM-Ppy/CC was further characterized at various scan rates of 10-100 mV/s (Figure 6b). As the scan rate increased, the POM-Ppy/CC maintained reversible and redox three peaks and had increased current densities, indicating potential of high rate capability.

The charge-discharge behavior of POM-Ppy/CC was intensively characterized using a galvanostatic charge-discharge measurement. Figure 7a showed charge-discharge profiles of POM-Ppy/CC measured at different current densities in the range of 1-30 mA/cm^2. These curves are symmetric, but non-linear due to the redox reactions of POMs which are consistent with CV characterization. The areal capacitance (mF/cm^2) was calculated from the discharge curves based on the following equation[4]:

$$C_{area} = I\triangle t/A\triangle V \quad (5)$$

where, I, $\triangle t$, A, and $\triangle V$ are the current (A), the discharge time (s), the potential window of the discharge (V), and the geometric surface area (cm^2), respectively. At low current density of 1 mA/cm^2, the POM-Ppy/CC had a maximum areal capacitance of 561 mF/cm^2. This result are much better than previously reported values from the Ppy-based electrode materials[24]. As the current density was increased to 30 mA/cm^2, the areal capacitance of the POM-Ppy/CC decreased slightly; 561 mF/cm^2 (1 mA/cm^2), 555 mF/cm^2 (2 mA/cm^2), 532 mF/cm^2 (5 mA/cm^2), 525 mF/cm^2 (7 mA/cm^2), 506 mF/cm^2 (12 mA/cm^2), 488 mF/cm^2 (20 mA/cm^2), and 476 mF/cm^2 (30 mA/cm^2), respectively. These high areal capacitance values were attributed to the combination of pseudocapacitive behavior of POM and Ppy and facilitated electron and ion transfer within 3D CC structures. These values were plotted in Figure 7b. The POM-Ppy/CC had a high level of 85% capacitance retention when increasing current densities from 1 to 30 mA/cm^2, indicating a high rate capability of POM-Ppy/CC.

In order to evaluate the durability of the POM-Ppy/CC, galvanostatic charge-discharge measurement was characterized at an applied constant current density of 1 mA/cm^2 under a three-electrode system over 1000 cycles. Figure 8 showed capacitance retention of the POM-Ppy/CC

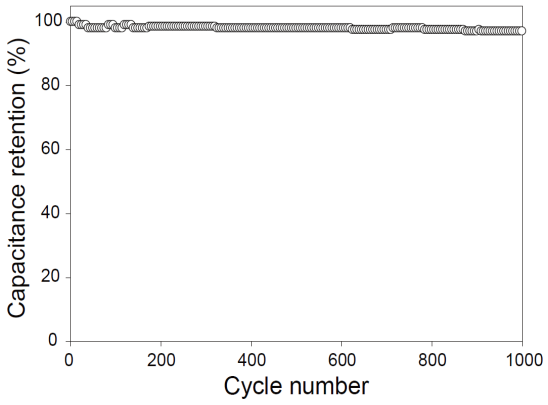

Figure 8. Cycling performance of POM-Ppy/CC measured at an applied constant current density of 1 mA/cm^2 during 1000 cycles.

during 1000 cycles. After 1000 cycles, capacitance fading was negligible; 97% capacitance retention was observed at the POM-Ppy/CC. This result indicated an excellent cycle life of the POM-Ppy/CC. The 3D CC structures effectively enhanced electron and ion transfer, and thus improved redox reactions of POM and Ppy over the long-term charge-discharge periods of time.

4. Conclusion

We prepared POM-doped Ppy-coated CC through a simple synthetic method of co-electrodeposition process and demonstrated its electrochemical behaviors in 1 M H_2SO_4 aqueous electrolyte. Coating amount of POM-Ppy was controlled by deposition times for a chronoamperometric technique; deposition time of 700 s was optimized. After optimization, the POM-Ppy/CC electrode exhibited excellent capacitive performances, such as, a high areal capacitance of 561 mF/cm^2 at 1 mA/cm^2, a high rate capability of 85% capacitance retention, and long-term cycling stability of 97% capacitance retention over 1000 cycles.

Acknowledgments

This work was supported by the National Research Foundation of Korea (NRF) Grant funded by the Korean Government (MSIP) (No. 2015R1C1A1A02036556).

References

1. C. Zhou, Y. Zhang, Y. Li, and J. Liu, Construction of high-capacitance 3D CoO@polypyrrole nanowire array electrode for aqueous asymmetric supercapacitor, *Nano Lett.*, **13**, 2078-2085 (2013).
2. T. Liu, L. Finn, M. Yu, H. Wang, T. Zhai, X. Lu, Y. Tong, and Y. Li, Polyaniline and polypyrrole pseudocapacitor electrodes with excellent cycling stability, *Nano Lett.*, **14**, 2522-2527 (2014).
3. L Yang, S. Cheng, Y. Ding, X. Zhu, Z. L. Wnag, and M. Liu, Hierarchical network architectures of carbon fiber paper supported cobalt oxide nanonet for high-capacity pseudocapacitors, *Nano Lett.*, **12**, 321-325 (2012).
4. M. Yang, S. B. Hong, and B. G. Choi, Hierarchical core/shell structure of MnO_2@polyaniline composites grown on carbon fiber paper for application in pseudocapacitors, *Phys. Chem. Chem. Phys.*, **17**, 29874-29879 (2015).
5. X. Zhao, B. M. Sánchez, P. J. Dobson, and P. S. Gran, The role of nanomaterials in redox-based supercapacitors for next generation energy storage devices, *Nanoscale*, **3**, 839-855 (2011).
6. S. Zhang, and N. Pan, Supercapacitors performance evaluation, *Adv. Energy Mater.*, **5**, 1401401-1401420 (2015).
7. K. Naoi, S. Ishimoto, J.-I. Miyamoto, and W. Naoi, Second generation 'nanohybrid supercapacitor': evoluation of capacitive energy storage devices, *Energy Environ. Sci.*, **5**, 9363-9373 (2012).
8. C.-C. Hu, K.-H. Chang, M.-C. Lin, and Y.-T. Wu, Design and tailoring of the nanotubular arrayed architecture of hydrous RuO_2 for next generation supercapacitors. *Nano Lett.*, **6**, 2690-2695 (2006).
9. M. M. P. Madrigal, F. Estrany, E. Armelin, D. D. Diaz, and C. Aleman, Towards sustainable solid-state supercapacitors: electroactive conducting polymers combined with biohydrogels, *J. Mater. Chem. A*, **4**, 1792-1805 (2016).
10. J. Cherusseri and K. K. Kar, Polypyrrole-decorated 2D carbon nanosheet electrodes for supercapacitors with high areal capacitance, *RSC Adv.*, **6**, 60454-60466 (2016).
11. K. Zhang, L. L. Zhang, X. S. Zhao, and J. Wu, Graphene/polyaniline nanofiber composites as supercapacitor electrodes, *Chem. Mater.*, **22**, 1392-1401 (2010).
12. S. Cho, K.-H. Shin, and J. Jang, Enhanced electrochemical performance of highly porous supercapacitor electrodes based on solution processed polyaniline thin films, *ACS Appl. Mater. Interfaces*, **5**, 9186-9193 (2013).
13. T. G. Yun, B. I. Hwang, D. Kim, S. Hyun, and S. M. Han, Polypyrrole-MnO_2-coated textile-based flexible-stretchable supercapacitor with high electrochemical and mechanical reliability, *ACS Appl. Mater. Interfaces*, **7**, 9228-9234 (2015).
14. C. Bora, J. Sharma, and S. Dolui, Polypyrrole/sulfnoated graphene composite as electrode material for supercapacitor, *J. Phys. Chem. C*, **118**, 29688-29694 (2014).
15. S. Biswas and L. T. Drzal, Multilayered nanoarchitecture of graphene nanosheets and polypyrrole nanowires for high performance supercapacitor electrodes, *Chem. Mater.*, **22**, 5667-5671 (2010).
16. F. F. D. Bélanger, Electropolymerization of polypyrrole and polyaniline-polypyrrole from organic acidic medium, *J. Phys. Chem. B*, **103**, 9044-9054 (1999).
17. D. Y. Liu and J. R. Reynolds, Dioxythiophene-based polymer electrodes for supercapacitor modules, *ACS Appl. Mater. Interfaces*, **2**, 3586-3593 (2010).
18. S. Chen and I. Zhitomirsky, Polypyrrole electrodes doped with sulfanilic acid azochromotrop for electrochemical supercapacitors, *J. Power Sources*, **243**, 865-871 (2013).
19. K. Shi and I. Zhitomirsky, Influence of current collector on capacitive behavior and cycling stability of tiron doped polypyrrole electrodes, *J. Power Sources*, **240**, 42-49 (2013).
20. M. Yang, B. G. Choi, S. C. Jung, Y.-K. Han, Y. S. Huh, and S. B. Lee, Polyoxometalate-coupled graphene via polymeric ionic liquid linker for supercapacitors, *Adv. Funct. Mater.*, **24**, 7301-7309 (2014).
21. M. Yang, D. S. Kim, J. H. Yoon, S. B. Hong, S. W. Jeong, D. E. Yoo, T. J. Lee, S. J. Lee, K. G. Lee, and B. G. Choi, Nanopillar films with polyoxometalate-doped polyaniline for electrochemical detection of hydrogen peroxide, *Analyst*, **141**,

1319-1324 (2016).
22. J. Hu, Y. Ji, W. Chen, C. Streb, and Y.-F. Song, "Wiring" redox-active polyoxometalates to carbon nanotubes using a sonication-driven periodic functionalization strategy, *Energy Environ. Sci.*, **9**, 1095-1101 (2016).
23. A. K. Cuentas-Gallegos, M. Lira-Cantú, N. Casañ-Pastor, and P. Gómez-Romero, Nanocomposite hybrid molecular materials for application in solid-state electrochemical supercapacitors, *Adv. Funct. Mater.*, **15**, 1125-1133 (2005).
24. G. M. Suppes, B. A. Deore, and M. S. Freund, Porous conducting polymer/heteropolyoxometalate hybrid material for electrochemical supercapacitor applications, *Langmuir*, **24**, 1064-1069 (2008).
25. N. Anwar, M. Vagin, F. Laffir, G. Armstrong, C. Dickinson, and T. McCormac, Transition metal ion-substituted polyoxometalates entrapped in polypyrrole as an electrochemical sensor for hydrogen peroxide, *Analyst*, **137**, 624-630 (2012).
26. Q. Cheng, J. Tang, J. Ma, H. Zhang, N. Shinya, and L.-C. Qin, Polyaniline-coated electro-etched carbon fiber cloth electrodes for supercapacitors, *J. Phys. Chem. C*, **115**, 23584-23590 (2011).
27. H. Wang and X. Wang, Growing nickel cobaltite nanowires and nanosheets on carbon cloth with different pseudocapacitive performance, *ACS Appl. Mater. Interfaces*, **5**, 6255-6260 (2013).
28. G. Bajwa, M. Genovese, and K. Lian, Multilayer polyoxometalates-carbon nanotube composites for electrochemical capacitors, *ECS J. Solid State Sci. Technol.*, **2**, M3046-M3050 (2013).